# Fine structure in the quadrupolar transition of the Ho $L_3$ pre-edge observed by lifetime-broadening-suppressed XANES spectroscopy

Hisashi Hayashi,* Masaki Kawata, Atsushi Sato, and Yasuo Udagawa
*IMRAM, Tohoku University, Katahira 2-1-1, Sendai 980-8577, Japan*
*and PRESTO, JST, 4-1-8 Honcho Kawaguchi, Saitama, 332-0012, Japan*

Toshiya Inami and Kenji Ishii
*SRRC, JAERI, Mikazuki, Hyogo, 679-5148, Japan*

Haruhiko Ogasawara
*Department of Physics, Northern Illinois University, DeKalb, Illinois 60115, USA*
*and APS, Argonne National Laboratory, 9700, South Cass Avenue, Illinois 60439, USA*

Susumu Nanao
*IIS, University of Tokyo, Komaba 4-6-1, Meguro, Tokyo 153-8505, Japan*
(Received 28 December 2004; published 12 July 2005)

The $2p3d$ resonant inelastic x-ray-scattering spectra of $Ho_2O_3$ are measured under 0.7 eV resolution and analyzed in terms of an equation based on the Kramers-Heisenberg formula. Broadening due to core-hole lifetime (4.26 eV) is completely suppressed to give sharp absorption bands with width of $<0.5$ eV together with energy position uncertainty $\sim 0.3$ eV. Observed bands are assigned to be well-known $2p \rightarrow 4f$ quadrupolar transitions that are otherwise buried under lifetime-broadened intense $2p \rightarrow 5d$ dipole transition. The present work opens up an opportunity to study $4f$-$5d$ interactions more accurately.

DOI: 10.1103/PhysRevB.72.045114 PACS number(s): 78.70.En, 61.10.Ht, 32.30.Rj

It has been well known that $L_3$ x-ray-absorption near-edge structure ($L_3$-XANES) is a direct probe of the electronic states in rare earth compounds.[1] The electronic structure of rare earth ions is governed by the interaction between electrons in the localized $4f$ orbitals and those in the broad $5d$ band.

In the $L_3$-XANES spectra, dominated by the contributions from the dipole allowed (E1) $2p \rightarrow 5d$ transition, quadrupolar (E2) $2p \rightarrow 4f$ transitions are expected to exist in the pre-edge region. Unfortunately, however, an inherent limitation due to core-hole lifetime broadening almost always prevents us from observing E2 transitions by x-ray-absorption spectroscopy.

Hence in the recent years considerable efforts have been devoted to extract $2p \rightarrow 4f$ transition components from overlapping $2p \rightarrow 5d$ transitions. Hämäläinen *et al.*[2] observed pre-edge structure by measuring the $2p3d$ ($L\alpha$) resonant inelastic x-ray scattering (RIXS) of $Dy(NO_3)_3$, where highly monochromatic incident x-ray energy is scanned across Dy $L_3$ edge while monitoring a narrow component of $L\alpha$ emission spectrum at a fixed energy. Bartolomé *et al.*[3,4] and Dallera *et al.*[5] tried to separate E2 transitions from dipolar ones by decomposition of a series of $L\alpha$ RIXS spectra obtained with various excitation energies. Journel *et al.*[6] simulated observed weak RIXS features using a schematic representation of the densities of unoccupied states. Krisch *et al.*[7] attempted to distinguish E2 transitions by $L\alpha$ RIXS excitation spectra where the energy transferred was kept constant. An elaborate deconvolution technique was also examined to extract the E2 component from high-quality conventional x-ray-absorption spectra.[8] Pre-edge E2 transitions are as important as E1 transitions in x-ray-magnetic circular dichroism (XMCD) spectra. Accordingly various efforts have been reported to observe E2 transitions by the use of XMCD spectra.[9–15]

Although these studies show that partial separation of E2 component is possible, none of them removes the core-hole lifetime broadening to accurately determine E2 transition energies and intensities. If removed, because of multiplet nature of the $4f$ states, the pre-edge is expected to show fine structures, which must provide us with much more detailed information about the $4f$-$5d$ interactions. Here we show lifetime broadening can be suppressed and fine structures in E2 transitions can be resolved by the analysis of, in principle, one high-resolution RIXS spectrum.

In previous papers[16,17] we have proposed a procedure that can deduce lifetime-broadening-suppressed (LBS)-XANES spectra from $1s2p$ ($K\alpha$) RIXS spectra of Cu through numerical analyses based on the Kramers-Heisenberg formula and have experimentally proved that LBS-XANES can, indeed, be retrieved. Subsequently, we have extended the approach to $L\alpha$ RIXS spectra of $Dy(NO_3)_3$ where final state effect arising from multiplet nature is significant[18] and have shown that a band due to $2p \rightarrow 4f$ quadrupole transitions is clearly separated from the tail of the intense white line. Because of a limited experimental resolution ($\sim 1.4$ eV), however, fine structures were not resolved. Theoretical RIXS spectra on several rare-earth compounds, where the effective resolutions are assumed to be 0.3 eV (Refs. 19 and 20) or 0.7 eV,[21,22] are rich in fine structure. Hence with improved resolution, much more structured RIXS and, accordingly, higher-resolution LBS-XANES spectra leading to better un-

 

derstanding of $4f$-$5d$ interactions are expected.

In this work $L\alpha$ RIXS spectra of $Ho_2O_3$ are studied under higher resolution than that employed in the previous work[18] in order to observe individual $2p \rightarrow 4f$ transitions separately. $Ho^{3+}$ $L\alpha$ emission was chosen because a detailed theoretical study about E2 transitions has been reported[20] and also because high-resolution measurements are feasible at around 6.7 keV, the Ho $L\alpha_1$ energy.

RIXS spectra were measured by using an x-ray spectrometer, which is specially designed for RIXS experiments and installed at the BL11XU beamline of SPring-8.[23] Here incident x-rays are monochromatized by two Si(111) and two Si(400) crystals to irradiate samples with the flux of about 10–12 photons/s. The spot size at the sample position was 0.15 mm (width) $\times$ 1.5 mm (height). The spectral width measured was $\sim$0.2 eV at 6.7 keV. The horizontally scattered x-rays were collected by a spherically bent Ge (531) crystal having a 2 m radius of curvature. The overall energy resolution in the present measurements was 0.7 eV as determined by the FWHM of elastic lines. All data were collected at room temperature at a constant scattering angle of $\sim 90°$ in the horizontal plane to avoid extraneous nonresonant scatterings. Conventional XANES spectra were obtained by monitoring total fluorescence while scanning the incident x-rays.

The analysis procedure employed here is based on an equation for the $L\alpha$ RIXS processes below,[18] which was originally derived for $1s2p$ transition by Tulkki and Åberg from the well-known Kramers-Heisenberg formula,[24]

$$\frac{d\sigma(\omega_1)}{d\omega_2} \propto \int \left\{ \frac{(\omega_2/\omega_1)(\Omega_{2p}+\omega) g_{3d,2p}(dg_{2p}/d\omega)}{(\Omega_{2p}+\omega-\omega_1)^2+\Gamma_{2p}^2/4\hbar^2} \right\} f_f(\omega_1-\omega_2 - \Omega_{3d}-\omega)d\omega. \quad (1)$$

Here $\omega_1$ and $\omega_2$ are incident and scattered photon energies, $\omega$ refers to the energies of the excited electrons in the intermediate state, and $\Gamma_{2p}$ is the width of the $2p$ level. The energies of $2p$ and $3d$ levels are represented by $\Omega_{2p}$ and $\Omega_{3d}$. The transition moment of the $L\alpha_1$ radiative transition is given by $g_{3d,2p}$, and $dg_{2p}/d\omega$ is the oscillator strength distribution for $L_3$ absorption, which is free from lifetime broadenings. $f_f(\omega_1-\omega_2-\Omega_{3d}-\omega)$ is a final state density function that ensures energy conservation. Our strategy is to make use of Eq. (1) to construct *one* (*true*) $dg_{2p}/d\omega$ that reproduces observed RIXS spectra at *every* excitation energy near the absorption threshold. Once established, a high-resolution RIXS spectrum would be enough to produce a LBS-XANES spectrum that reflects density of states.

For application of Eq. (1) to Ho $L\alpha_1$ RIXS, the function $f_f(\omega_1-\omega_2-\Omega_{3d}-\omega)$ must be appropriately determined. Reflecting the multiplet nature of the final states, the Ho $L\alpha_1$ band is asymmetric. The Ho $L\alpha_1$ band was measured well above the $L_3$ edge and fitted with a function consisting of four Lorentzians. Subsequently, each Lorentzian was deconvoluted by a Lorentzian with FWHM=$\Gamma_{2p}$ and the resultant components were added together to make $f_f$ functions. The value of $\Gamma_{2p}$ was set at 4.26 eV.[25] Shown in Fig. 1 is the $f_f$ profile determined for Ho $L\alpha_1$ together with a schematic representation of the scattering process. The instrumental resolution function as well as finite lifetime broadening of

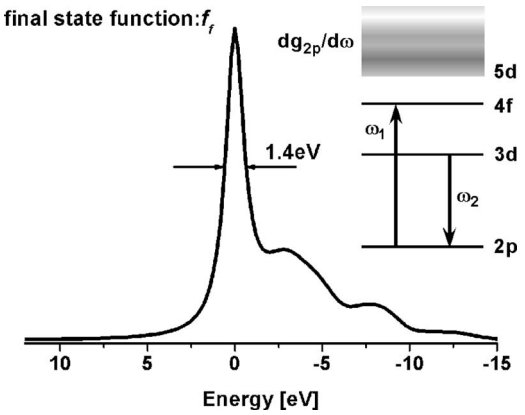


FIG. 1. Assumed final state density function $f_f$ for 0.7 eV-resolution study regenerated from four Lorentzians fitted to the $L\alpha_1$ emission of $Ho_2O_3$. Inset is a schematic of the $L\alpha$ RIXS process.

the final states has been involved in the $f_f$. The FWHM of the main peak in the $f_f$ is $\sim$1.4 eV, which is clearly larger than the instrumental resolution ($\sim$0.7 eV). Thus the instrumental resolution effects on $f_f$ are expected to be small, and hence the final state broadening determines the effective resolution of the present RIXS spectra. As described below, even under this limited resolution, it was found that, if the width of two bands in LBS-XANES separated by $\sim$1 eV of each other is broadened by $\sim$0.5 eV, a discernible difference is brought about in the corresponding RIXS spectra.

RIXS measurements were performed at the excitation energies of 8042.4, 8059.3, and 8062.8 eV. Squares in Fig. 2(a) represent a whole RIXS spectrum excited at 8062.8 eV, where the abscissa is the energy transferred ($\Delta E=\omega_1-\omega_2$). Four features, indicated by A, B, A′, and B′, are evident. The energy position and overall band shape of the band B is very similar to that reported as E2 RIXS on $Ho_2Fe_{14}B$, where measurements were made with 1–1.5 eV resolution.[4] In Fig. 2(b) the band B region of the RIXS spectra excited at 8062.8, 8059.3, and 8042.4 eV is presented in an expanded scale. Fine structures are clearly observed in every spectrum at the same energy losses; $\Delta E \sim 1341.1(B_1)$, $\sim 1342.1(B_2)$, $\sim 1343.8(B_3)$, and though less distinct, $\sim 1345.7$ eV($B_4$). The relative energies from $B_1$ are 1.0($B_2$), 2.7($B_3$), and 4.6 eV($B_4$), respectively. A theoretical calculation of the E2 part of the RIXS signals has been reported on Ho by van Veenendaal *et al.*[20] These values are in good agreement with calculated ones, namely, 1.0($B_2$), 3.0($B_3$), and 5.0 eV($B_4$), although the $\Delta E$ values graphically estimated from Ref. 20 show systematic deviations of $\sim$2 eV: 1343.2($B_1$), $\sim 1344.2(B_2)$, $\sim 1346.2(B_3)$, and $\sim 1348.2$ eV($B_4$).

Attempted next is to deduce the best-fit $dg_{2p}/d\omega$ that reproduces each RIXS spectrum by the use of Eq. (1). To begin with, a conventional XANES spectrum, which is shown in Fig. 3(a), was assumed to represent $dg_{2p}/d\omega$ and RIXS spectra were calculated. Differences between the observed and, thus, calculated RIXS spectra were considerable. Subsequently, calculations by Eq. (1) were repeated by modifying $dg_{2p}/d\omega$ by trial and error in order to make the observed and calculated RIXS spectra agree. In the course of the analysis it

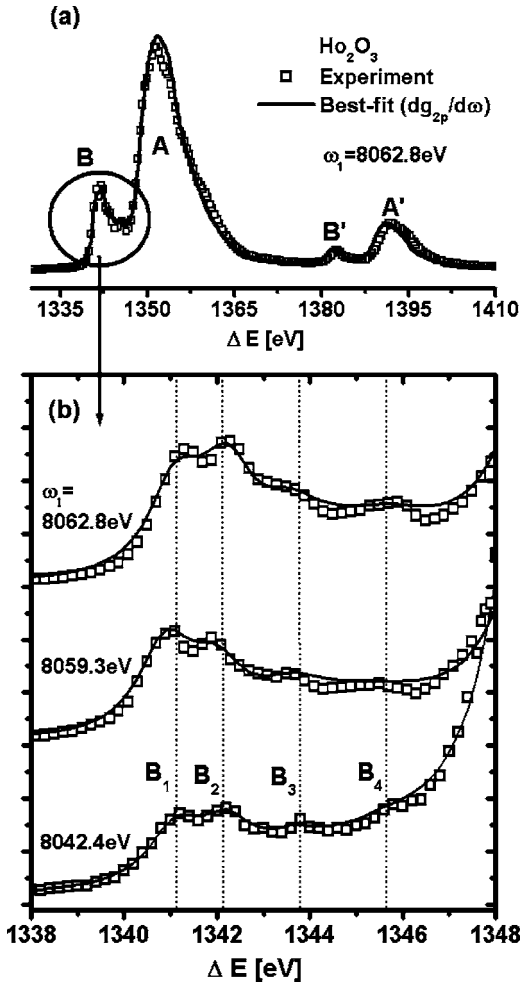


FIG. 2. (a) Open squares: $L\alpha$ RIXS spectra of $Ho_2O_3$ obtained for 8062.8 eV excitation. Solid line: calculated RIXS spectra by the use of the best-fit $dg_{2p}/d\omega$ for 8062.8 eV excitation data. The abscissa is the transferred energy $\Delta E=\omega_1-\omega_2$. (b) Open squares: RIXS spectra of band B region excited with 8062.8, 8059.3, and 8042.4 eV in an expanded scale. Solid line: calculated RIXS spectra by the use of respective best-fit $dg_{2p}/d\omega$ shown in Fig. 3(b).

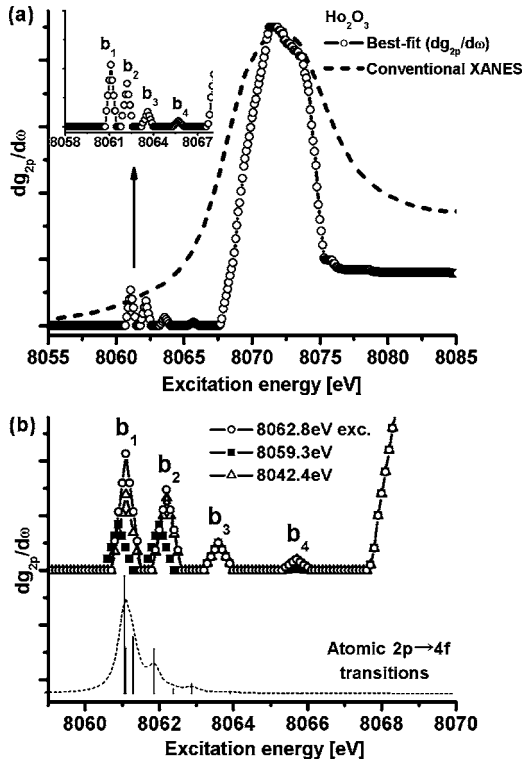


FIG. 3. (a) Conventional $L_3$-XANES spectrum of $Ho_2O_3$ (broken line), and the best-fit $dg_{2p}/d\omega$ determined from the 8062.8 eV excitation RIXS (circles). The inset is the pre-edge part in an expanded scale. (b) Upper: pre-edge part of $dg_{2p}/d\omega$ profiles that reproduces $L\alpha$ RIXS spectra shown in Fig. 2(b); open circles (8062.8 eV exc.), solid squares (8059.3 eV exc.), and open triangles (8042.4 eV exc.). Lower: the calculated $dg_{2p}/d\omega$ for the $2p\rightarrow 4f$ quadrupolar transitions in $Ho^{3+}$ ion (bars). Also plotted is the convolution of the calculated $dg_{2p}/d\omega$ by Lorentzians with 0.4 eV width (broken line).

has turned out that a presence of four very sharp pre-edge absorption bands is essential to reproduce RIXS fine structures in Fig. 2(b). Shown in Fig. 3(a) is the $dg_{2p}/d\omega$ that best reproduces the RIXS spectrum obtained with 8062.8 eV excitation. The four bands are indicated by $b_1-b_4$, and each corresponds to the features $B_1-B_4$ in Fig. 2, respectively. These bands are concluded to be due to E2 transitions because of their energies and low intensities. Ho E2 transition has been studied by Bartolomé *et al.* from decomposition of a series of low-resolution RIXS spectra.[4] Although a second discrete feature was not identified, they noted that resonance takes place at two energies. Their observation indicates an existence of several discrete E2 bands below the E1 transition, which we have just confirmed.

The energies of the features in Fig. 2(b) are very sensitive to the energies of the pre-edge bands; a shift of a pre-edge peak by $\sim$0.3 eV makes a discernible change in the energy of the corresponding RIXS feature. Bandwidths of these bands must be $<$0.5 eV; if larger, the features $B_1-B_4$ get obscured. As long as the integrated intensity remains unchanged, smaller bandwidth does not affect the band shapes of $B_1-B_4$ very much. In Fig. 3, the bandwidths of the pre-edge bands are taken to be 0.4 eV. A drastic improvement of $dg_{2p}/d\omega$ in resolution by high-resolution RIXS analysis is evidenced when compared to the conventional XANES spectrum. The solid line in Fig. 2(a) is the RIXS-spectrum-generated from the $dg_{2p}/d\omega$ shown in Fig. 3(a). It almost perfectly overlaps with the observed RIXS spectrum.

In Fig. 3(b) shown are $dg_{2p}/d\omega$'s deduced individually from the three RIXS spectra in an expanded scale. Only the pre-edge part is presented because above 8067 eV the spectra are almost the same. These $dg_{2p}/d\omega$'s are normalized by the peak intensity of the white line. Calculated RIXS spectra from each $dg_{2p}/d\omega$ are shown by solid lines in Fig. 2(b), where agreements between the observed spectra and calculated ones are satisfactory. The peak energies and integrated intensities of the four bands $b_1-b_4$ determined from the three RIXS spectra are given in Table I together with estimated errors. Here intensity is normalized as the intensity of the main peak at 8071.5 eV to be 1. The error values in Table I mean that if the peak energies or integrated intensities are increased or decreased by these values, calculated RIXS

TABLE I. Peak energies and relative intensities of bands $b_1-b_4$ deduced from $L\alpha$ RIXS spectra obtained at the excitation energies 8042.4, 8059.3, and 8062.8 eV.

| Excitation energy (eV) | $b_1$ | $b_2$ | $b_3$ | $b_4$ |
|---|---|---|---|---|
| 8042.4 | 0.031±0.004 | 0.028±0.005 | 0.011±0.004 | 0.004±0.004 |
| | 8061.1±0.2 | 8062.2±0.2 | 8063.6±0.3 | 8065.7±0.3 |
| 8059.3 | 0.019±0.002 | 0.018±0.004 | 0.011±0.004 | 0.001±0.001 |
| | 8060.9±0.2 | 8062.0±0.2 | 8063.6±0.3 | 8065.7±0.4 |
| 8062.8 | 0.047±0.005 | 0.033±0.004 | 0.011±0.003 | 0.004±0.004 |
| | 8061.1±0.1 | 8062.2±0.1 | 8063.6±0.3 | 8065.7±0.3 |

spectra show definitely discernible differences. Thus although our final goal to construct *one* $dg_{2p}/d\omega$ that reproduces *every* RIXS spectrum is not fully achieved, multiplet structures are clearly resolved and their energies determined with uncertainty of $<0.3$ eV. On the other hand, ambiguity in intensity is somewhat larger, and an existence of $b_4$ band in Fig. 3 is marginal. One of the reasons lies in insufficient S/N ratio of the RIXS spectra as will be noted from Fig. 2(b). The dispersions in the table can be regarded to represent uncertainties in energy and intensity deduced from the procedure presented here.

For comparison, the $dg_{2p}/d\omega$ for the $2p \rightarrow 4f$ quadrupolar transitions in $Ho^{3+}$ ion, which was calculated by Cowan's program,[26] are indicated by bars in Fig. 3(b). Also shown by dots is their convolution by Lorentzians with 0.4 eV width. In this calculation, Coulomb parameters obtained within the Hartree-Fock limit were reduced to 80% to account for intraatomic screening effects. The scales of both energy and intensity are relative. The energy range and overall tendency in the strength distribution roughly agree with the observation, which is another proof that the bands $b_1-b_4$ are E2 transitions. A close look of Fig. 3(b) tells us, however, that there are some differences between the experimental $dg_{2p}/d\omega$ and the calculated one. For example, relative intensities of high-energy bands are stronger and the energy separations are wider than the calculated results. The reason of the disagreements is not clear at this stage. It may be due to chemical effects, which are completely neglected in the present calculation, or may suggest that theories beyond Eq. (1), where interferences between intermediate states are neglected, must be employed.[27] Detailed analyses of such effects in the LBS-XANES are subjects for future studies.

In conclusion, we have experimentally proved that fine structures in E2 transitions buried under lifetime-broadened E1 transition can be revealed from analyses of high-resolution $L\alpha$ RIXS spectra. Transition energies can be determined within 0.3 eV from the RIXS measurements at 0.7 eV resolution. Compared to other procedures to extract E2 transitions discussed in the introductory section, the present approach has a definite advantage to determine transition energies separately and precisely because of core-hole lifetime-broadening suppression. For high-resolution measurements, analyzer crystals should be used at high Bragg angles. This imposes some experimental restriction, but a suitable crystal planes of Si or Ge can be found for most elements [e.g., Ge(440) for Dy, Ge(531) for Ho, and Si(531) for Er]. Hence the present approach can be widely applied to study weak forbidden states buried under strong broad transition, E2 transitions of all lanthanide elements being one of the cases.

## ACKNOWLEDGMENTS

The experiments were carried out at SPring-8 under the Proposal No. 2003B0144-NXa-np. Discussion with Professor A. Kotani of JASRI is greatly acknowledged. One of the authors (H.O.) is supported by the US Department of Energy.

*Corresponding author. Electronic address: hayashi@tagen.tohoku.ac.jp

[1] A. Kotani, T. Jo, and J. C. Parlebas, Adv. Phys. **37**, 37 (1988).
[2] K. Hämäläinen, D. P. Siddons, J. B. Hastings, and L. E. Berman, Phys. Rev. Lett. **67**, 2850 (1991).
[3] F. Bartolomé, J. M. Tonnerre, L. Sève, D. Raoux, J. Chaboy, L. M. García, M. Krisch, and C.-C. Kao, Phys. Rev. Lett. **79**, 3775 (1997).
[4] F. Bartolomé, M. H. Krisch, D. Raoux, and J.-M. Tonnerre, Phys. Rev. B **60**, 13497 (1999).
[5] C. Dallera, M. H. Krisch, A. Rogalev, C. Gauthier, J. Goulon, F. Sette, and A. Sole, Phys. Rev. B **62**, 7093 (2000).
[6] L. Journel, J.-M. Mariot, J.-P. Rueff, C. F. Hague, G. Krill, M. Nakazawa, A. Kotani, A. Rogalev, F. Wilhelm, J.-P. Kappler *et al.*, Phys. Rev. B **66**, 045106 (2002).
[7] M. H. Krisch, C. C. Kao, F. Sette, W. A. Caliebe, K. Hämäläinen, and J. B. Hastings, Phys. Rev. Lett. **74**, 4931 (1995).
[8] P. W. Loeffen, R. F. Pettifer, S. Müllender, M. A. van Veenendaal, J. Röhler, and D. S. Sivia, Phys. Rev. B **54**, 14877 (1996).
[9] P. Fischer, G. Schutz, and S. Stahler, J. Appl. Phys. **69**, 6144 (1991).
[10] J. C. Lang, G. Srajer, C. Detlefs, A. I. Goldman, H. Konig, X. Wang, B. N. Harmon, and R. W. McCallum, Phys. Rev. Lett. **74**, 4935 (1995).
[11] M. H. Krisch, F. Sette, U. Bergmann, C. Masciovecchio, R. Verbeni, J. Goulon, W. Caliebe, and C. C. Kao, Phys. Rev. B **54**,

R12673 (1996).
[12] J. Chaboy, F. Bartolomé, L. M. Garcia, and G. Cibin, Phys. Rev. B **57**, R5598 (1998).
[13] C. Giorgetti, E. Dartyge, F. Baudelet, and C. Brouder, Appl. Phys. A: Mater. Sci. Process. **73**, 703 (2001).
[14] H. Wende, Z. Li, A. Scherz, G. Ceballos, K. Baberschke, A. Ankudinov, J. J. Rehr, F. Wilhelm, A. Rogalev, D. L. Schlagel *et al.*, J. Appl. Phys. **91**, 7361 (2002).
[15] T. Nakamura, H. Shoji, E. Hirai, S. Nanao, K. Fukui, H. Ogasawara, A. Kotani, T. Iwazumi, I. Harada, R. Katano *et al.*, Phys. Rev. B **67**, 094439 (2003).
[16] H. Hayashi, R. Takeda, Y. Udagawa, T. Nakamura, H. Miyagawa, H. Shoji, S. Nanao, and N. Kawamura, Phys. Rev. B **68**, 045122 (2003).
[17] H. Hayashi, R. Takeda, M. Kawata, Y. Udagawa, Y. Watanabe, T. Takano, S. Nanao, N. Kawamura, T. Uefuji, and K. Yamada, J. Electron Spectrosc. Relat. Phenom. **136**, 199 (2004).
[18] H. Hayashi, R. Takeda, M. Kawata, Y. Udagawa, N. Kawamura, Y. Watanabe, and S. Nanao, Phys. Rev. B **70**, 155113 (2004).
[19] P. Carra, M. Fabrizio, and B. T. Thole, Phys. Rev. Lett. **74**, 3700 (1995).
[20] M. van Veenendaal, P. Carra, and B. T. Thole, Phys. Rev. B **54**, 16010 (1996).
[21] S. Tanaka, K. Okada, and A. Kotani, J. Phys. Soc. Jpn. **63**, 2780 (1994).
[22] M. Nakazawa, K. Fukui, H. Ogasawara, A. Kotani, and C. F. Hague, Phys. Rev. B **66**, 113104 (2002).
[23] T. Inami, T. Fukuda, J. Mizuki, H. Nakao, T. Matsumura, Y. Murakami, K. Hirota, and Y. Endoh, Nucl. Instrum. Methods Phys. Res. A **467–468**, 1081 (2001).
[24] J. Tulkki and T. Åberg, J. Phys. B **15**, L435 (1982).
[25] M. O. Krause and J. H. Oliver, J. Phys. Chem. Ref. Data **8**, 329 (1979).
[26] R. D. Cowan, *The Theory of Atomic Structure and Spectra* (University of California Press, Berkeley, 1981).
[27] T. Lebrun, *Raman Emission by X-Ray Scattering* (World Scientific, Singapore, 1996).